Phase Offset Based Channel Estimation Method for Optical OFDM/OQAM Systems

Xi Fang, *Member, IEEE*, Yueyang Yu, Hua Jiang, Xianwei Gao, Lei Zhang, Lifang Liu, and Ding Ding

***Abstract*— In this letter, we developed a novel phase offset (PHO)-based channel estimation method for optical orthogonal frequency division multiplexing (OFDM)/offset quadrature amplitude modulation (OQAM). In this approach, the suppression of intrinsic imaginary interference (IMI) induced by both the linear and nonlinear impairment could be improved by increasing the pseudo pilot power with the using of PHO. As demonstrated in the numerous Montel Carlo simulation results, PHO outperforms the interference approximation methods (IAMs) for both the suppressing IMI and combating the fiber nonlinearity induced interference.**

***Index Terms*— OFDM/OQAM, channel estimation, pseudo pilot, IMI.**

I. Introduction

COMPARED to conventional orthogonal frequency division multiplexing (OFDM), OFDM offset quadrature amplitude modulation (OFDM/OQAM) could be a promising candidate for the next generation optical communication system since it enables high spectral efficiency by eliminating the cyclic prefix (CP), and a lower out of band leakage by utilizing filter banks with promising time-frequency localization (TFL) property [1]. However, the orthogonal condition for OFDM/OQAM only holds in the real field, resulting in that the chromatic dispersion (CD) and polarization mode dispersion (PMD) might lead to serious intrinsic imaginary interference (IMI) to optical OFDM/OQAM [2], evidently deteriorating the system performance and lead to bit-error-rate (BER) floor.

To overcome the obstacle of IMI, numerous studies have tended to concentrate on the channel estimation (CE) for optical OFDM/OQAM [2]. In [3], Zhao proposed time domain CE method for single polarization optical OFDM/OQAM. In [2], frequency domain CE based on IMI approximating has been discussed for coherent OFDM/OQAM. In [4], time domain least square algorithm demonstrated improved performance compared with [2]. In [5], frequency domain averaging method has been proved effective in combating IMI for intensity-modulation direct detection (IMDD) OFDM/OQAM. In [6], orthogonal basis expansion based method has been studied for combating IMI induced by phase noise. The methods in [3], [4], [6] were based on time domain transmission model, the complexities for which tend to be serious due to the requiring of matrix inversion. The proposal in [2], [7] utilized the concept of interference approximation method (IAM) to decrease CE complexity. For IAM, the concept of pseudo pilots has been utilized to improve CE accuracy by extracting IMI from the received pilots. However, [5] is designed for IM-DD system and could not be directly applied for coherent OFDM/OQAM, research in [2] lacks of the discussion on the designing of pilot preambles to achieve optimal CE performance. For wireless OFDM/OQAM, a series of IAM variants were presented [7], including IAM-R, IAM-I and IAM-C. Unfortunately, for the IAMs, residual interference becomes significant at poor optical signal-to-noise ratio (OSNR) since the IMI distributed outside of first order time-frequency neighbor zoom being totally ignored. To our best knowledge, discussions on the designing of pilot preambles for the obtaining of optimal CE performance have not been reported for optical OFDM/OQAM to date.

In this paper, we present a novel phase offset (PHO) based CE method for optical OFDM/OQAM. The mathematic derivation indicates that IMI could be suppressed most effectively when the optimal pilot power was obtained by using PHO. As validated by numerical simulation results, the proposed PHO method outperforms the IAMs in both suppressing IMI and nonlinear induced interference evidently.

II. Theoretical Model

The schematic diagram of optical OFDM/OQAM is shown in Fig.1. Baseband OFDM/OQAM signal in the discrete time domain [2] is expressed as:

$$s(k) = \sum_{n}\sum_{m=0}^{N-1} a_{m,n}\, g\left(k - n\frac{N}{2}\right) e^{j2\pi mk/N} e^{j\frac{\pi}{2}(m+n)}. \quad (1)$$

where N is the number of sub-carriers in an OFDM/OQAM block, $a_{m,n}$ is the real-valued data of the mth sub-carrier on the nth block. Phase modulation $\phi_{m,n} = (m+n)\cdot\pi/2$ is employed to guarantee the real field orthogonal condition. In (1), $g(k)$ denotes the impulse response of the prototype filter.

The signal traverses the optical fiber with an impulse response of $h(l)$. For the facility of discussion, the received signal without considering the laser phase noise and nonlinear effect could be given by:

$$\begin{aligned} r(k) &= \sum_{l} h(l)\, s(k-l) + \omega(k) \\ &= \sum_{l}\sum_{n}\sum_{m=0}^{N-1}\left[a_{m,n}\, g\left(k - l - n\frac{N}{2}\right) e^{j\frac{2\pi m(k-l)}{N}} \right. \\ &\quad \left. \times\, e^{j\frac{\pi}{2}(m+n)}\cdot h(l)\right] + \omega(k) \\ &= \sum_{l}\sum_{n}\sum_{m=0}^{N-1}\left[a_{m,n}\, g\left(k - n\frac{N}{2}\right)\right. \\ &\quad \left. \times e^{j\frac{2\pi m(k-l)}{N}} e^{j\frac{\pi}{2}(m+n)}\cdot h(l)\right] + \omega(k) \end{aligned} \quad (2)$$

Manuscript received May 29, 2019; revised June 18, 2019; accepted June 24, 2019. Date of publication June 28, 2019; date of current version July 17, 2019. This work was supported in part by the National Natural Science and Foundation of China under Grant 61701008, in part by the Fundamental Research Funds for the Central Universities of China under Grant 328201802 and 328201913, and in part by the Beijing-Central University Co-Construction Research Project (Advanced Research on DSP for 5G Communication). *(Corresponding authors: Lei Zhang; Ding Ding.)*

The authors are with the Beijing Electronics Science and Technology Institute, Beijing 100070, China (e-mail: zhanglei@besti.edu.cn; dingding@besti.edu.cn).

Color versions of one or more of the figures in this letter are available online at http://ieeexplore.ieee.org.

Digital Object Identifier 10.1109/LPT.2019.2925662

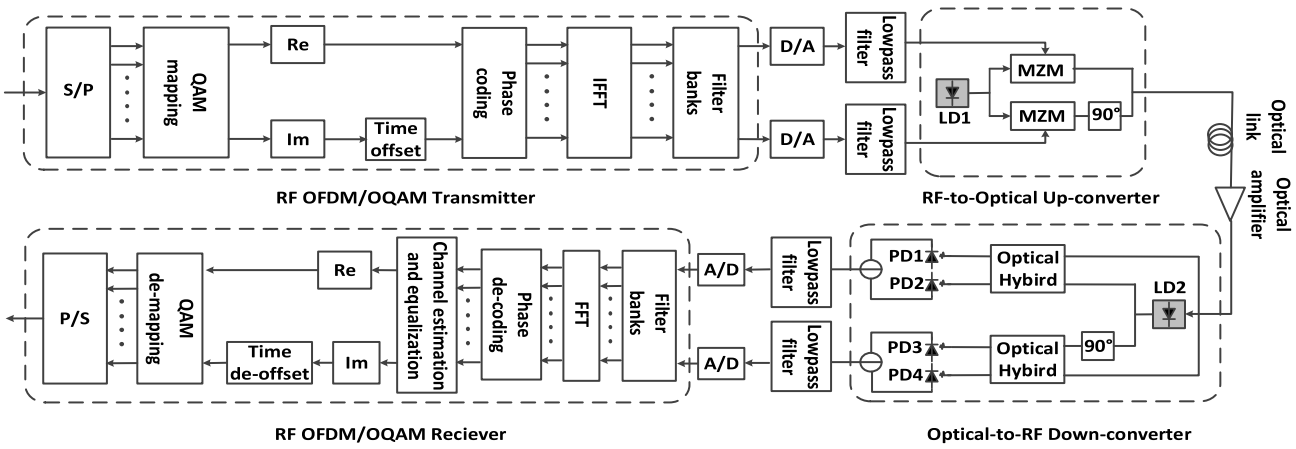

Fig. 1. Schematic diagram of optical OFDM/OQAM system. S/P: serial-to-parallel conversion. P/S: parallel-to-serial conversion. D/A: digital-to-analogue conversion. A/D: analogue-to-digital conversion. LD: local diode. MZM: Mach-Zehnder modulator. PD: photo detector.

where $\omega(k)$ is the amplified spontaneous emission (ASE) noise. Under the condition $1/T_g$ is less than the coherence bandwidth of the channel $B_c = 1/2\Delta$, we could assume $g(k)$ has relatively low variations over time interval $t \in [0, \Delta]$ as $g\left(k-l-n\frac{N}{2}\right) \approx g\left(k-n\frac{N}{2}\right)$. Here T_g denotes the length of the prototype filter and Δ stands for the maximum delay spread of the channel [2]. For OFDM/OQAM, T_g is usually several times the length of symbol period and Δ is usually small for this system. The demodulated signal $d_{m,n}$ can be written as:

$$\begin{aligned} & d_{m,n} \\ &= \sum_k r(k)\, g^*\left(k-n\frac{N}{2}\right) e^{-j\frac{2\pi mk}{N}} e^{-j\frac{\pi}{2}(m+n)} \\ &= \sum_k \sum_l \sum_p \sum_q \{a_{m+p,n+q}\, g\left(k-(n+q)\frac{N}{2}\right) g^*\left(k-n\frac{N}{2}\right) \\ &\quad \times e^{j\frac{2\pi(m+p)(k-l)}{N}} e^{j\frac{\pi(m+p+n+q)}{2}} e^{-j\frac{2\pi mk}{N}} e^{-j\frac{\pi(m+n)}{2}} \cdot h(l)\} + \omega_{m,n} \\ &= \sum_s \sum_l \sum_{(p,q)} a_{m+p,n+q}\, g\left(s+\frac{Nq}{4}\right) g\left(s-\frac{Nq}{4}\right) \\ &\quad \times e^{j\frac{2\pi(m+p)}{N}\left(s+\frac{Nn}{2}+\frac{Nq}{4}-l\right)} e^{j\frac{\pi(m+p+n+q)}{2}} e^{-j\frac{2\pi m}{N}\left(s+\frac{Nn}{2}+\frac{Nq}{4}\right)} \\ &\quad \times e^{-j\frac{\pi(m+n)}{2}} h(l) + \omega_{m,n} \\ &= a^{(c)}_{m,n} H_{m+p} + \omega_{m,n} \end{aligned} \tag{3}$$

Pseudo pilot $a^{(c)}_{m,n}$ is defined as:

$$\begin{aligned} a^{(c)}_{m,n} &= a_{m,n} \\ &\quad + \underbrace{\sum_{(p,q)\in\Omega^*_{(1,1)}} a_{m+p,n+q} \cdot j^{p+q+p(q+2n)} \cdot A_g(-q\tau,-p\upsilon)}_{a^{IMI}_{m,n}}. \end{aligned} \tag{4}$$

and $A_g(-q\tau,-p\upsilon)$ is the ambiguity function [2] defined as:

$$A_g(-q\tau,-p\upsilon) = \sum_s g\left(s+\frac{Nq}{4}\right) g\left(s-\frac{Nq}{4}\right) \times e^{j\frac{2\pi}{N}ps}. \tag{5}$$

where τ and υ are the time and frequency interval between consecutive blocks and sub-carriers, equal to $N/2$ and $1/N$, respectively. Here, $\Omega^*_{(1,1)} = \{(p,q)\,||p| \le 1, |q| \le 1, (p,q) \ne (0,0)\}$ is the first order neighbor zone in the frequency-time plane excluding the basic data point. In addition, $H_{m+p} = \sum_l h(l)\, e^{-j\frac{2\pi(m+p)l}{N}}$ denotes the channel frequency response. In the derivation of (3), we have utilized assumption $H_{m+p} \approx H_{m,n}$ for $\Omega^*_{(1,1)}$. With (3), CE could be processed as:

$$\widehat{H}_{m,n} = \frac{d_{m,n}}{a^{(c)}_{m,n}} = \frac{a^{(c)}_{m,n} H_{m,n} + \omega_{m,n}}{a^{(c)}_{m,n}} = H_{m,n} + \frac{\omega_{m,n}}{a^{(c)}_{m,n}}. \tag{6}$$

According to (6), promoting the power of the pseudo pilot $a^{(c)}_{m,n}$ could improve the CE performance by suppressing the interference induced by $\omega_{m,n}$ and other residual interference.

III. Phase Offset Based CE Method

In this section, PHO based CE method is discussed to achieve optimal performance by maximizing the power of pseudo pilot. Based on (4), the power of the pseudo pilot can be expressed as:

$$\begin{aligned} E\left(\left|a^{(c)}_{m,n}\right|^2\right) &= E\left(\left|a_{m,n}\right|^2\right) + E\left(\left|a^{IMI}_{m,n}\right|^2\right) \\ &= \sigma_p^2 + \sigma_p^2 \sum_{(p,q)\in\Omega^*_{1,1}} \left|a_{m+p,n+q} \left\langle g_{m,n}, g_{m+p,n+q}\right\rangle\right|^2 \end{aligned} \tag{7}$$

where $E(\cdot)$ denotes the power, σ_p^2 is the variance of the real-valued pilot symbol $a_{m,n}$. $\left\langle g_{m,n}, g_{\mathrm{m+p,n+q}}\right\rangle = j^{p+q+p(q+2n)} A_g(-q\tau,-p\upsilon)$ is the interference weight of the filter banks. According to [8], $A_g(\cdot)$ shows a centrosymmetric property, i.e., $A_g(-q\tau,-p\upsilon) = A_g(-q\tau, p\upsilon)$ and $A_g(-q\tau,-p\upsilon) = A_g(q\tau,-p\upsilon)$. For $(p,q) \notin \Omega_{(1,1)}$, $A_g(-q\tau,-p\upsilon)$ approaches to zero. Consequently, the pseudo pilot has the following weights matrix in $\Omega_{(1,1)}$

$$W = \begin{bmatrix} jc & ja & jc \\ -jb & 1 & jb \\ jc & -ja & jc \end{bmatrix}. \tag{8}$$

Here, the row and the column vectors referring to the time and frequency respectively, a, b, c are real valued parameter, which could be previously calculated off line.

For PHO, we employed three consecutive OFDM/OQAM blocks as the preamble and placed nulls in the first and third blocks to reduce the CE complexity, i.e., $a_{m,n-1} = a_{m,n+1} = 0$. Then, the pilot in the center block $a_{m+i,n}$, $i \in \{1, 2, \ldots N\}$ was utilized. With $e^{j\theta} = \cos\theta + j\sin\theta$, the pilot power was normalized as $E\left(\left|a_{m+i,n}\right|^2\right) = 1$. In this case, preamble A could be written as

$$A = \begin{bmatrix} 0 & e^{j\theta_{m+1,n}} & 0 \\ 0 & e^{j\theta_{m,n}} & 0 \\ 0 & e^{j\theta_{m-1,n}} & 0 \end{bmatrix}. \tag{9}$$

where $\theta_{m,n}$, $\theta_{m+1,n}$ and $\theta_{m-1,n}$ denote the phases of three consecutive pilot symbols respectively and $\theta_{m+i,n} \in [-\pi, \pi)$. With (8) and (9), (4) is then simplified as

$$\begin{aligned} a_{m,n}^{(c)} &= a_{m,n} + j^{-1-2n} a_{m-1,n} A_g(0,-\nu) + j^{1+2n} a_{m+1,n} A_g(0,\nu) \\ &= a_{m,n} + A_g(0,\nu)(j^{-1-2n} a_{m-1,n} + j^{1+2n} a_{m+1,n}) \\ &= \begin{cases} e^{j\theta_{m,n}} + a \cdot j \cdot (e^{j\theta_{m-1,n}} - e^{j\theta_{m+1,n}}) & n = odd \\ e^{j\theta_{m,n}} + a \cdot j \cdot (e^{j\theta_{m+1,n}} - e^{j\theta_{m-1,n}}) & n = even \end{cases}. \end{aligned} \tag{10}$$

In case n is an odd number integer, $a_{m,n}^{(c)}$ is expressed as:

$$\begin{aligned} a_{m,n}^{(c)}\Big|_{n=odd} &= \cos\theta_{m,n} - a\sin\theta_{m-1,n} + a\sin\theta_{m+1,n} \\ &\quad + j(\sin\theta_{m,n} + a\cos\theta_{m-1,n} - a\cos\theta_{m+1,n}) \end{aligned} \tag{11}$$

Thus, the power of pseudo pilots is given by

$$\begin{aligned} &E\left(\left|a_{m,n}^{(c)}\right|^2\right) \\ &= \left|\mathrm{Re}(a_{m,n}^{(c)})\right|^2 + \left|\mathrm{Im}(a_{m,n}^{(c)})\right|^2 \\ &= 1 + 2a^2 - 2a^2\cos(\theta_{m-1,n} - \theta_{m+1,n}) \\ &\quad + 2a\sin(\theta_{m,n} - \theta_{m-1,n}) + 2a\sin(\theta_{m+1,n} - \theta_{m,n}) \end{aligned} \tag{12}$$

From (12), the optimal pseudo pilot power will be achieved when $\theta_{m,n}$, $\theta_{m+1,n}$ and $\theta_{m-1,n}$ satisfying PHO as

$$\theta_{m-1,n} - \theta_{m+1,n} = -\pi. \tag{13}$$

$$\theta_{m,n} - \theta_{m-1,n} = \frac{\pi}{2}. \tag{14}$$

$$\theta_{m+1,n} - \theta_{m,n} = \frac{\pi}{2}. \tag{15}$$

Substituting the (13) to (15) into (9), the general structure of the preamble when n is an odd integer could be given as (16). In, considering the periodicity of trigonometric function, we construct each pilot module with four pilots to guarantee the constant power of each pilot module.

$$A_{odd} = \begin{bmatrix} 0 & e^{j\theta_{m,n}+\frac{\pi}{2}} & 0 \\ 0 & e^{j\theta_{m,n}} & 0 \\ 0 & e^{j\theta_{m,n}-\frac{\pi}{2}} & 0 \\ 0 & e^{j\theta_{m,n}-\pi} & 0 \end{bmatrix}. \tag{16}$$

Repeating the analysis discussed above, we obtain the general structure of the preamble when n is an even integer as

$$A_{even} = \begin{bmatrix} 0 & e^{j\theta_{m,n}-\frac{\pi}{2}} & 0 \\ 0 & e^{j\theta_{m,n}} & 0 \\ 0 & e^{j\theta_{m,n}+\frac{\pi}{2}} & 0 \\ 0 & e^{j\theta_{m,n}+\pi} & 0 \end{bmatrix}. \tag{17}$$

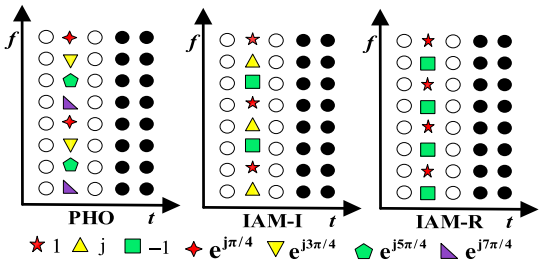

Fig. 2. The pilot structure for PHO, IAM-I and IAM-R.

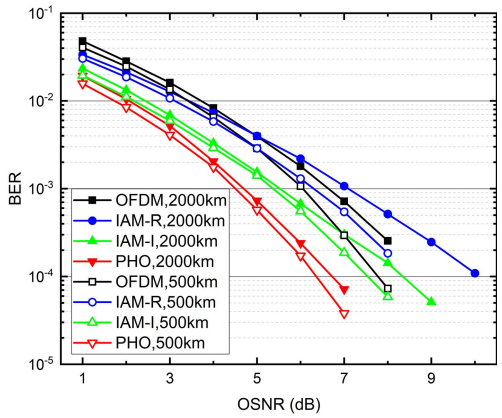

Fig. 3. Comparison of the BER performance of optical OFDM/OQAM using PHO, IAMs, and optical OFDM in linear transmission with 10GS/s sampling rate.

IV. Simulation Results and Discussion

In this section, numerical simulations were conducted by using the commercial software VPI transmissionMaker 9.9 to validate the advantage of PHO. IAM-I and IAM-R were simulated as comparisons for PHO. Pilot structures for the three methods were depicted in Fig.2. Each OFDM/OQAM block was generated by 256 point FFT, for which 216 data sub-carriers were loaded with OQAM symbols, 20 null sub-carriers were allocated in the middle to avoid the energy fading, each 5 null sub-carriers were placed in the both two sides as guard interval, 10 pilot sub-carriers were periodically inserted for the facility of phase correction. Each OFDM/OQAM frame contained 300 OFDM/OQAM blocks and the first three blocks were used as the pilot preambles. Considering all the redundancy for pilots, preambles and 7% overhead for forward error correction, the net and raw bit rate for the optical OFDM/OQAM, with 10GS/s sampling rate, were 15.32 Gb/s and 16.39 Gb/s, respectively. The occupied bandwidth was 8.83 GHz. Thus, the net and raw spectral efficiency were 1.74 bit/s/Hz and 1.86 bit/s/Hz. Both DAC and ADC were assumed with unlimited bandwidth and without quantization noise. Isotropic orthogonal transform algorithm (IOTA) filter with length of 1024 was utilized in constructing the filter banks. The fiber link consisted of several spans of 100km standard single mode fiber (SSMF) with an average loss of 20 dB each. An Erbium-doped fiber amplifier (EDFA) fully compensated the fiber attenuation in each span. The fiber dispersion was 17ps/km/nm. Laser linewidth has been assumed ideal in this paper for the convenience of discussion.

Fig.3. shows the BER performance of IAMs, PHO, and optical OFDM in linear transmission scenarios. We set CP size for optical OFDM as 60, to accommodate CD induced interference

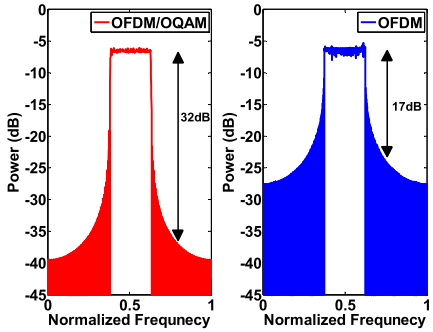

Fig. 4. Comparison of the emitted spectrum of optical OFDM/OQAM and optical OFDM at the transmitter side.

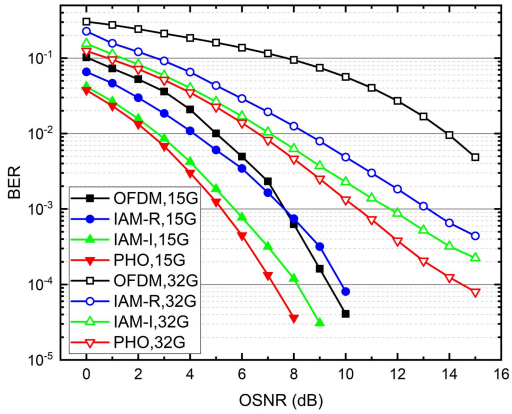

Fig. 5. Comparison of the BER performance of optical OFDM/OQAM using PHO, IAMs and optical OFDM in 500km linear transmission for different sampling rate.

in 2000km transmission. The nonlinear index was zero in this part. The bandwidth for the transmitter was 10GHz. In the receiver, super-Gaussian optical filter with 3dB bandwidth of 10GHz was utilized. The electrical signals were then filtered by a 5th–order low-pass Bessel filter with 3dB bandwidth of 7.5GHz. The OSNR, with 12.5GHz bandwidth for noise power measurement, was controlled by feeding appropriate ASE noise at the receiver. As shown in Fig.3, at 10^{-3} BER, PHO outperforms IAM-I by 1dB and IAM-R by 2dB in OSNR penalty for 500km transmission. The advantage of PHO is more evident in 2000km transmission due to better IMI robustness of PHO, thanks to the obtaining of optimal pseudo pilot power. The performance of PHO obviously outperforms optical OFDM in linear transmission. This is mainly due to lower out-of-band leakage of the optical OFDM/OQAM. As shown in the emitted spectrum of the transmitter in Fig.4, optical OFDM/OQAM demonstrates 15dB out-of-band leakage advantage compared with optical OFDM thanks to the promising TFL property of the filter banks.

Fig.5 shows the performance of PHO and IAMs in 500km linear transmission with different sampling rate. As shown in Fig.5, at 32GS/s sampling rate, the accumulation of IMI is more serious. In this case, the advantage of PHO is more obvious thanks to the improved robustness against IMI.

Fig.6 depicts the capability of the PHO and the IAM-R in combating the fiber nonlinearity induced interference. In this part, the fiber nonlinear index is 1.32/W/km, the noise figure of the EDFA is 5dB. The noise bandwidth has been

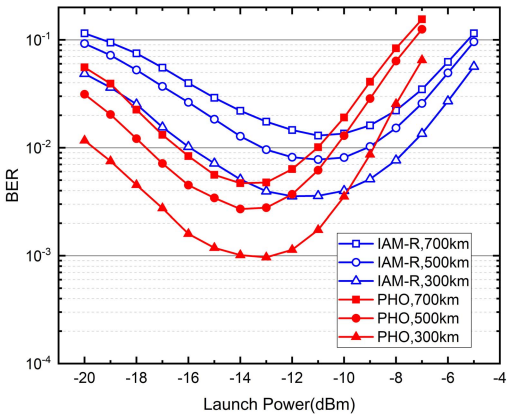

Fig. 6. Comparison of the BER performance of PHO, IAM-R in nonlinear transmission with 10GS/s sampling rate.

assumed unlimited. As shown in Fig.6, the BER performance of PHO outperform IAM-R with the launch power varies from −20dBm to -5dBm, after 300km, 500km and 700km transmissions. In 700km transmission, the optimal launch power for PHO and IAM-R are −13dBm and −11dBm, respectively. 2dBm launch power improvement could be obtained with the using of PHO. For the promising TFL property of optical OFDM/OQAM, nonlinear induced interference is mainly brought by $a_{m+p,n+q}$ $\left((p,q) \in \Omega_{(1,1)}\right)$, while interference from $a_{m+p,n+q}$ $\left((p,q) \notin \Omega_{(1,1)}\right)$ could be effectively suppressed. Channel estimation and equalization accuracy in nonlinear transmission scenarios could be evidently improved thanks to the promoting of pseudo pilot power brought by PHO.

V. Conclusion

A novel PHO based channel estimation method for optical OFDM/OQAM has been proposed in this paper. The simulation results show that PHO outperforms the IAMs for both suppressing IMI and combating the nonlinear interference evidently thanks to the promoting of pseudo pilot power.

References

[1] Q. Yang, Z. He, Z. Yang, S. Yu, X. Yi, and W. Shieh, "Coherent optical DFT-Spread OFDM transmission using orthogonal band multiplexing," *Opt. Express*, vol. 20, no. 3, pp. 2379–2385, 2012.

[2] X. Fang, Y. Xu, Z. Chen, and F. Zhang, "Frequency-domain channel estimation for polarization-division-multiplexed CO-OFDM/OQAM systems," *J. Lightw. Technol.*, vol. 33, no. 13, pp. 2743–2750, Jul. 1, 2015.

[3] Z. Jian, "Channel estimation in DFT-based offset-QAM OFDM systems," *Opt. Express*, vol. 22, no. 21, pp. 25651–25662, 2014.

[4] X. Fang, Y. Xu, Z. Chen, and F. Zhang, "Time-domain least square channel estimation for polarization-division-multiplexed CO-OFDM/OQAM systems," *J. Lightw. Technol.*, vol. 34, no. 3, pp. 891–900, Feb. 1, 2015.

[5] L. Zhang, S. Xiao, M. Bi, L. Liu, and Z. Zhou, "Channel estimation algorithm for interference suppression in IMDD–OQAM–OFDM transmission systems," *Opt. Commun.*, vol. 364, pp. 129–133, Apr. 2016.

[6] X. Fang, C. Yang, T. Zhang, and F. Zhang, "Orthogonal basis expansion-based phase noise suppression for PDM CO-OFDM system," *IEEE Photon. Technol. Lett.*, vol. 26, no. 4, pp. 376–379, Feb. 15, 2014.

[7] W. Liu, D. Chen, D. Kong, and T. Jiang, "Preamble overhead reduction with IAM-C for channel estimation in OQAM-OFDM systems," in *Proc. IEEE ChinaSIP*, 2015, pp. 761–765.

[8] S. Kang and K. Chang, "A novel channel estimation scheme for OFDM/OQAM-IOTA system," *ETRI J.*, vol. 29, no. 4, pp. 430–436, 2007.